Absence of Observable Biotin−Protein Interactions in the 1.3S Subunit of Transcarboxylase: An NMR Study†

D. Venkat Reddy,‡ Bhami C. Shenoy,§ Paul R. Carey,§ and Frank D. Sönnichsen*,‡

Department of Physiology and Biophysics and Department of Biochemistry, Case Western Reserve University, Cleveland, Ohio 44106

Received July 10, 1997; Revised Manuscript Received September 30, 1997⊗

ABSTRACT: Transcarboxylase (TC) is a biotin-containing enzyme catalyzing the transfer of a carboxyl group from methylmalonyl-CoA to pyruvate to form propionyl-CoA and oxalacetate. The transfer is achieved *via* carboxylated biotin bound to a 1.3S subunit within the multisubunit enzyme complex. The 1.3S subunit of TC is a 123 amino acid polypeptide, to which biotin is covalently attached at Lys 89. We have overexpressed 1.3S in *Escherichia coli* and characterized the biotinylated and apo-forms by 1D- and 2D-NMR spectroscopy. To search for protein−biotin interactions, which could modulate the reactivity of the biotin ring on the 1.3S subunit, we have compared the chemical shifts, relaxation parameters, and NH exchange rates of the ureido ring protons of free and 1.3S-bound biotin. These properties are similar for both forms of the biotin. Further, NOE experiments on 1.3S revealed no detectable cross peaks between biotin and the protein. Consistent with these findings, the 2D NMR data for holo- and apo-1.3S are essentially identical indicating little or no changes in conformation between the two forms of the protein. The conclusion that strong protein−biotin interactions do not exist in 1.3S contrasts with the findings for the biotin carboxylase carrier protein from *E. coli* acetyl-CoA carboxylase, which reveal significant biotin−protein contacts [Athappilly, F. K., and Hendrickson, W. A. (1995) *Structure 3*, 1407−1419]. Further, the biotin NH1′ exchange rates determined for 1.3S show that in the region of optimal activity for TC (pH 5.5−6.5) acid-catalyzed exchange predominates. In this pH range the base-catalyzed rate is too small (<1 s^{-1}) to account for the turnover rate of the enzyme. Thus, the means by which the N1′ atom is activated for nucleophilic attack of the carboxyl group in methylmalonyl-CoA does not appear to depend on interactions within the 1.3S subunit alone; rather activation must occur at the interfaces of the subunits in the holoenzyme.

Biotin (Figure 1) is the essential cofactor for those enzymes that transfer units of carbon dioxide in metabolic pathways. Within these proteins, biotin functions as a carrier of the CO_2 moiety. Biotin-containing enzymes are found throughout the living world and are important in human well-being. Four biotin-containing carboxylases are involved in the carbon chain elongation steps in mammalian metabolism, i.e., in gluconeogenesis, fatty acid synthesis, propionate metabolism, and in the catabolism of leucine (*1*).

Transcarboxylase (TC)[1] from *Propionibacterium shermanii* occupies a unique position among biotin-containing enzymes because it catalyzes the transfer of a carboxyl group from methylmalonyl-CoA to pyruvate to form propionyl-CoA and oxalacetate without the involvement of free CO_2, HCO_3^-, or ATP (*2*). TC is a complex, multi-subunit enzyme of M_r = 1200K, composed of 30 polypeptide chains of three different subunits types (1.3S, 5S, and 12S). In the intact form of TC, there are a total of six 12S monomers in a cylindrical central unit, twelve 5S monomers in six dimeric outer 5S subunits, and twelve 1.3S subunits. The latter subunit of the TC is the biotin carboxyl carrier unit and consists of a 123 amino acid (12.6 kDa) polypeptide chain. Biotin is covalently attached to the Lys 89 ϵ-amino group of 1.3S as a post-translational modification by holo-carboxylase synthetase (*3*). The 1.3S subunit has two key roles: first, it provides regions for binding the central and outer subunits of the enzyme, and second, in the enzymatic reaction its biotin serves as carboxyl group carrier. In the first partial reaction at the interface of the 1.3S and 12S subunits a COO^- group is transferred from methylmalonyl-CoA to the biotin ring:

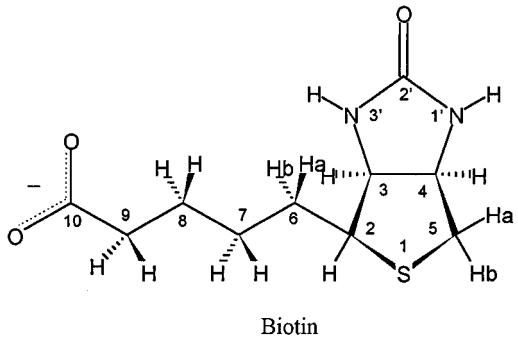

Biotin

FIGURE 1: Numbering scheme in biotin.

† The present study was supported by a Research Initiation Grant of the Ohio Board of Regents (F.D.S.) and NIH Grant DK5305301 (P.R.C. and F.D.S.).

* Author to whom correspondence should be addressed. Telephone: (216) 368-5405. Fax: (216) 368-1693. E-mail: frank@herring.phol.cwru.edu.

‡ Department of Physiology and Biophysics.

§ Department of Biochemistry.

⊗ Abstract published in *Advance ACS Abstracts,* November 15, 1997.

[1] Abbreviations: ATP, adenosine triphosphate; DSS, 4,4-dimethyl-4-silapentane-1-sulfonate; 1D, one-dimensional; 2D, two-dimensional; DQF-COSY, double-quantum filtered correlation spectroscopy; NOE, nuclear Overhauser effect; NOESY, nuclear Overhauser enhancement spectroscopy; TOCSY, total correlation spectroscopy; TC, transcarboxylase.

S0006-2960(97)01674-7 CCC: $14.00

$$CH_3CH(COO^-)COSCoA + 1.3S{-}biotin \overset{12S\ subunit}{\rightleftharpoons} CH_3CH_2COSCoA + 1.3S{-}biotin{-}COO^- \quad (1)$$

The biotin then translocates to the interface between the 1.3S and 5S subunits, and the COO^- species is taken up by pyruvate to form oxalacetate:

$$1.3S{-}biotin{-}COO^- + CH_3COCOO^- \overset{5S\ subunit}{\rightleftharpoons} {}^-OOCCH_2COCOO^- + 1.3S{-}biotin \quad (2)$$

In the entire carboxylase family of enzymes biotin can be viewed as the vehicle to carry and deliver carbon dioxide (*4*). The structural and electronic properties of the biotin molecule itself, which facilitate these roles, have been the subject of much attention from chemists and biochemists (*5*−*12*). The enzymatic carboxylation of *d*-biotin involves the replacement of the N1′ ureido proton by a carboxyl group. Knowles (*13*) has reviewed the work which addresses the problem of how the N1′ position of the biotin ring becomes carboxylated in view of the low nucleophilicity of that nitrogen. Especially pertinent are the observations of Mildvan and co-workers (*14*), confirmed and refined by Perrin and Dwyer (*15*) that the exchange of biotin ureido NH protons with water occurs at rates comparable to the rate of enzyme-catalyzed carboxylation of biotin. Thus, at neutral pH and higher, base catalyzed exchange of the ureido NH protons can generate a nucleophilic N^- species at a rate high enough to account for the rate of biotin carboxylation.

In the present work we measured the exchange rates of the ureido NH protons for biotin on the 1.3S protein. They resemble closely those found for free biotin. In addition, there are close parallels in other NMR properties of free and 1.3S-bound biotin. Thus, we find no evidence for 1.3S−protein−biotin interactions activating the N1′ position for nucleophilic attack. It is therefore likely that activation of the N1′ atom for attack toward CO_2 is a property of the interface between 1.3S and 12S subunits.

MATERIALS AND METHODS

Sample Preparation. DSS and D_2O were purchased from Cambridge Isotope Laboratories (Andover, MA), and *d*-biotin was purchased from Sigma Chemical Company (St. Louis, MO). The recombinant 1.3S subunit was expressed in *Escherichia coli* and purified according to Shenoy et al. (*16*), using affinity chromatography on an avidin-monomeric agarose column and by C8 reverse phase HPLC. *E. coli* cells were grown on minimal M-9 media with added biotin to improve the yield of the biotinylated form of 1.3S. The biotinylated 1.3S (holo-protein) and the apo-1.3S subunit, both of which bind to the avidin column, were separated on an ether-5PW column using hydrophobic interaction chromatography, yielding about 10 mg of holo-1.3S and 30 mg of apo-1.3S per liter of medium.

NMR Spectroscopy. NMR experiments were carried out on a Varian Unity Plus spectrometer operating at a proton frequency of 600 MHz. Approximately 10 mg of lyophilized holo- or apo-1.3S were dissolved in 500−600 μL of 90% H_2O/10% D_2O (v/v) to yield ∼1.5 mM protein solutions. For comparison 0.6 mg of *d*-biotin was dissolved in 600 μL of 90% H_2O/10% D_2O (v/v) to give an approximately 4 mM solution. In each case, DSS (0.1 mM) was added as an internal standard.

Two-dimensional DQF-COSY (*17*, *18*), TOCSY (*19*, *20*), and NOESY (*21*−*23*) experiments were carried out at 20 °C and at pH 6.9 for holo-1.3S and at pH 6.5 for apo-1.3S. Mixing times of 50 ms in TOCSY and 350 ms in NOESY experiments were used. Usually, 16−32 transients with a relaxation delay of 1.5 s were collected for each FID. A sweep width of 6600 Hz was used in both $F2$ and $F1$ dimensions. The acquired data consisted of 2048 data points in $F2$ and 256−300 complex data points in the $F1$ dimension. The data were zero filled to give a spectrum of 4096 × 2048 data points after Fourier transformation. Shifted sine bell window functions were applied in both dimensions. All spectra were referenced to the signals of the methyl group protons of DSS (0.0 ppm).

The ^{1}H 1D NMR variable temperature experiments on holo-1.3S and free biotin were carried out from 5 to 50 °C. For each spectrum 64 transients were collected with a presaturation delay of 1.5 s.

Determination of Biotin Ureido NH Proton Exchange Rates. The hydrogen exchange rates of the biotin ureido ring NH protons were measured by the saturation-transfer technique and selective T_1 measurements of the individual proton resonances (*14*, *15*, *24*) for free biotin and protein-bound biotin. When the exchange rate (k_{ex}) between the labile amide proton and water is equal to or faster than its spin−lattice relaxation rate ($1/T_1$), saturation of the solvent resonance will reduce the intensity of the exchangeable proton resonance according to eq 3:

$$\text{fractional amide intensity } (I_1/I_0) = 1/(1 + k_{ex}T_1) \quad (3)$$

where I_1 and I_0 are the NH proton intensities in the presence and absence of solvent irradiation, respectively. Similarly, the measured relaxation rate ($1/T_1^{obs}$) will be greater than the intrinsic rate ($1/T_1$) according to eq 4:

$$1/T_1^{obs} = 1/T_1 + k_{ex} \quad (4)$$

The $1/T_1$ can be calculated from measured fractional amide proton intensities and relaxation rates ($1/T_1^{obs}$) by using eqs 3 and 4. Since hydrogen exchange is acid- and base-catalyzed, measurement of the pH dependence of the fractional amide intensity gives acid- and base-catalyzed rate constants k_{H^+} and k_{OH^-}, respectively, by eq 5:

$$k_{ex} = k_{H^+}[H_3O^+] + k_{OH^-}[OH^-] \qquad \text{or}$$

$$k_{ex} = k_{H^+} \times 10^{-pH} + k_{OH^-} \times 10^{pH-pK_W}$$

$$\log k = \log(k_{H^+}[H^+] + 0.68092 \times 10^{-14}k_{OH^-}/[H^+]) \quad (5)$$

with pK_W being the ionic product of water at 20 °C.

The T_1 values were measured by an inversion−recovery method, using symmetrically-shifted shaped pulses (SS pulses) for the 90° observation pulse, as well as for the 180° inversion pulse. This method allowed us to invert both biotin NH protons selectively without excitation of the water signal and thereby helped to suppress the large water signal (*25*). The fractional amide intensities were measured again using SS pulses for a 90° observation pulse in 1D-NMR experiments with and without presaturation, and 128 scans were

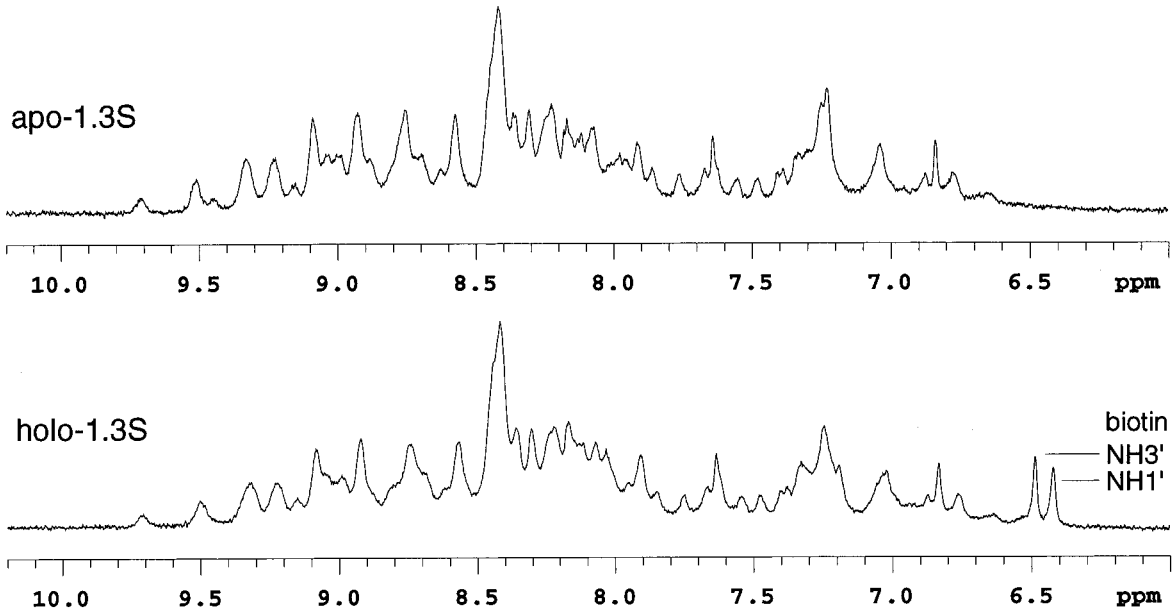

FIGURE 2: Comparison of amide proton region of 1D spectra of apo- and holo-1.3S proteins at 20 °C in 90% H_2O/10% D_2O (v/v) and pH 6.4 and 6.5, respectively, showing close similarities in two forms of the protein. The biotin ureido NH proton resonances in the holo-protein are labeled and are absent in the apo-protein.

acquired for each spectrum with a delay of 1.5 s. pH titrations were carried out at 20 °C, from pH 4.50 to 8.12 for holo-1.3S protein and from 4.63 to 7.94 for free biotin. Each time the sample pH was adjusted with small amounts of DCl or NaOD, and after the NMR measurements the pH stability was verified with a pH microelectrode (Microelectrodes Inc., Bedford, NH) that fits into the NMR tube. Reported pH values were not corrected for deuterium isotope effects.

RESULTS AND DISCUSSION

Similarities between Ureido NH Protons in Free Biotin and in 1.3S

^{1}H Chemical Shifts and Connectivities. A partial ^{1}H 1D NMR spectrum of holo-1.3S is shown in Figure 2. The resonance dispersion in this region and in the aliphatic region (not shown) indicates the folded nature of the protein. The figure further demonstrates that biotin's ureido protons, NH1′ and NH3′, are separated from the protein amide region, resonating at 6.42 and 6.48 ppm, respectively. These and the remaining biotin−proton resonance assignments in the 1.3S−biotin complex (Table 1) were determined using ^{1}H−^{1}H homonuclear 2D DQF-COSY and 2D TOCSY experiments.

With few exceptions, the chemical shifts observed for the biotin moiety in 1.3S are identical within experimental error to those of free biotin determined here (Table 1), or previously reported (*26*). Due to the covalent linkage to the protein, i.e. the amidification of biotin's carboxyl group with Lys 89 in 1.3S, 8H2, and 9H2 are shifted by 0.04 and 0.06 ppm, respectively. Similarly, the chemical shift difference ($\Delta\delta$) between the ureido protons NH3′ and NH1′ is reduced to 0.07 ppm versus 0.13 ppm in free biotin (Table 1). This reduction in $\Delta\delta$ also originates in the amidification of biotin's carboxyl group, as methyl ester formation already reduces the $\Delta\delta$ to 0.08 ppm (*14*). This observation has been attributed to a sterically caused reduction in the propensity for an intramolecular hydrogen bond formation between biotin's carboxyl group and the NH3′. The chemical shift data provide the first indication that the biotin on the protein is not being perturbed significantly by the protein.

Table 1: ^{1}H NMR Chemical Shifts (δ, ppm) for Biotin and 1.3S−Biotin in 90% H_2O/10% D_2O (v/v) at 20 °C and pH 6.5 and 6.9, Respectively[a]

proton	biotin	1.3S−biotin	$\Delta\delta$(1.3S−biotin−biotin)
NH3′	6.52	6.48	−0.04
NH1′	6.39	6.42	0.03
3H	4.44	4.42	−0.02
4H	4.60	4.60	0.00
5Ha	3.00	2.97	−0.03
5Hb	2.77	2.76	−0.01
2H	3.35	3.32	−0.03
6Ha	1.71	1.72	0.01
6Hb	1.59	1.58	−0.01
7H2	1.41	1.40	−0.01
8H2	1.60	1.64	0.04
9H2	2.19	2.25	0.06

[a] The chemical shifts are measured with respect to the internal DSS at 0 ppm. The error in the chemical shift measurement is ±0.01 ppm.

An expanded region of the 2D NOESY spectrum, showing the NOE connectivities between the biotin ureido protons NH1′ and NH3′, and other protons in the protein−biotin complex, is given in Figure 3a. The NH1′ shows strong NOE cross peaks with the 4H, 5Hb ring protons and weak NOEs with the 3H, 5Ha ring protons and the 7H2 and 8H2 side-chain protons. At the same time, NH3′ shows strong NOE cross peaks with the 3H ring proton, the 6Hb side-chain proton, and weak NOEs with the 6Ha and 7H2 side-chain protons. Figure 3b shows an expansion of the 2D NOESY spectrum which includes the ureido NH−amide NOE interactions in the protein−biotin complex. Under the experimental conditions employed, NOEs with the biotin ureido protons would be expected to be observed for any stable biotin−protein interactions that involve short proton−proton distances. However, no such NOE cross peaks were observed indicating the absence of significant interactions between the biotin ureido ring and the protein backbone. All

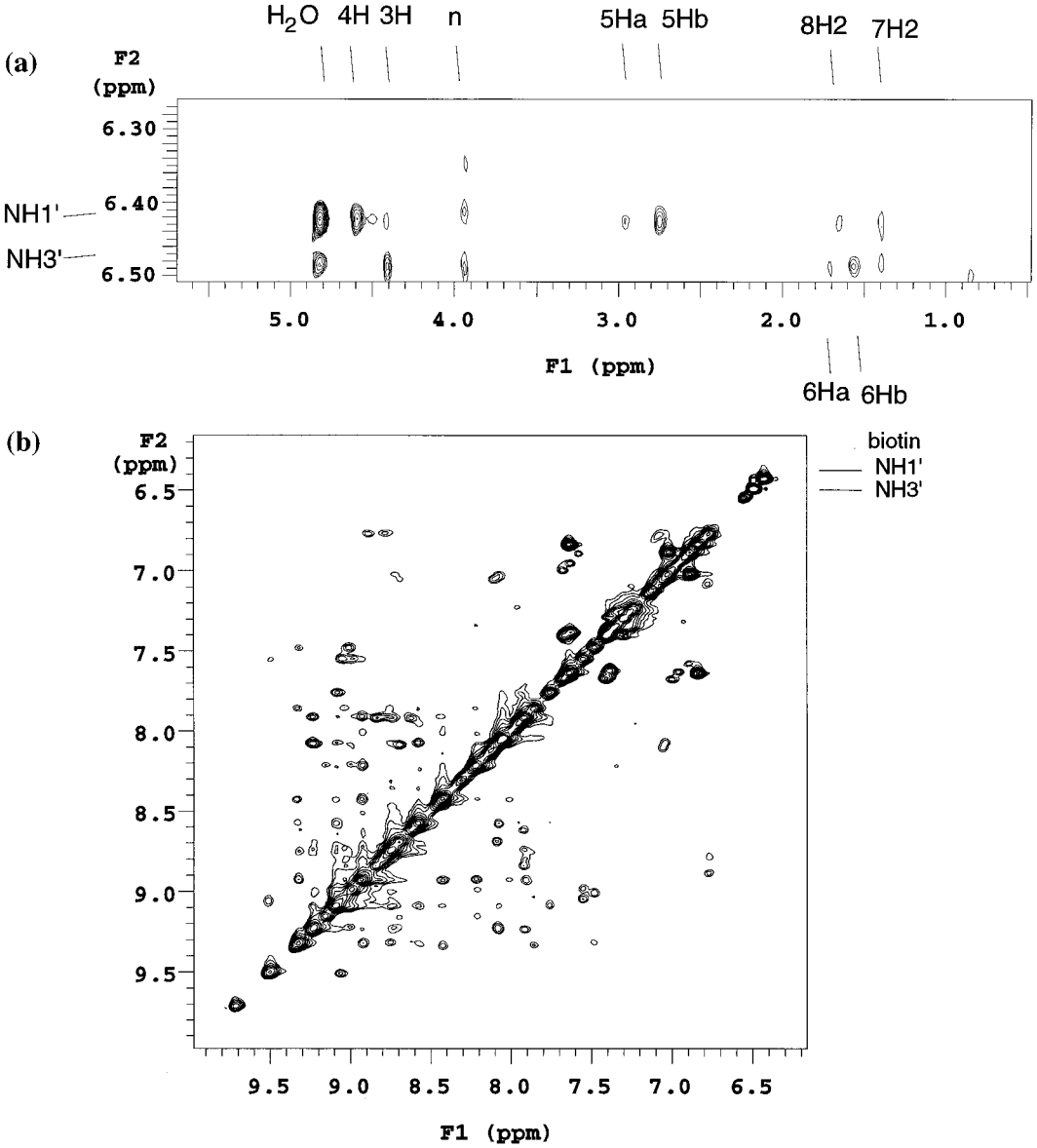

FIGURE 3: 2D $^1H-^1H$ NOESY spectra of holo-1.3S protein at pH 6.9 and 20 °C in 90% H_2O/10% D_2O (v/v). (a) Expanded region shown includes through space correlations between biotin ureido NH protons and aliphatic protons; the intraresidual NOEs within the biotin are labeled, "n" indicates noise. (b) Expanded region containing amide−amide NOE interactions in the protein showing that the biotin ureido NH protons have no detectable NOEs with the protein amide protons.

Table 2: Summary of Proton-Exchange Measurements and Temperature Coefficients $\Delta\delta/\Delta T$ for Ureido NH Protons for Free Biotin and 1.3S−Biotin at 20 °C in 90% H_2O/10% D_2O (v/v)[a]

	biotin		1.3S−biotin	
	NH1′	NH3′	NH1′	NH3′
T_1 (s)	1.90	1.80	0.95	0.85
k_{H^+} (M^{-1} s^{-1})	1.8 (±0.06) × 10^6	0.4 (±0.02) × 10^6	2.8 (±0.1) × 10^6	0.2 (±0.01) × 10^6
k_{OH^-} (M^{-1} s^{-1})	5.0 (±0.2) × 10^7	0.9 (±0.07) × 10^7	4.3 (±0.2) × 10^7	1.1 (±0.05) × 10^7
$\Delta\delta/\Delta T$ (ppb/°C, at pH 6.5)	−5.8	−6.7	−5.8	−6.7

[a] Errors in measurement of T_1 values are ±0.05 s. The exchange rates were obtained by nonlinear least-squares fitting of the pH dependence of biotin NH proton exchange data to eq 5, using T_1 values in the Table. Errors in the calculation of exchange rates are given in parentheses.

the NOEs involving the biotin NHs were found to be exclusively intraresidual, i.e. between the NHs and other protons on the biotin cofactor.

NH Exchange Rates of Biotin. The hydrogen-exchange rates of the biotin ureido protons NH1′ and NH3′ were obtained for a range of pH values for the free biotin and the protein-bound biotin. Figure 4 shows a plot of the rate constants vs pH for biotin bound to 1.3S and for free biotin. The data were fitted with a nonlinear least-squares procedure to obtain rate constants (Table 2). For the free biotin the rate constants are in agreement with the values obtained by Perrin and Dwyer (*15*). In comparison to free biotin, the acid-catalyzed rate constants for NH1′ and NH3′ in the 1.3S−biotin complex show a 50% increase and decrease, respectively. However, for the base-catalyzed exchange only small changes (20%) are seen for the two ureido protons.

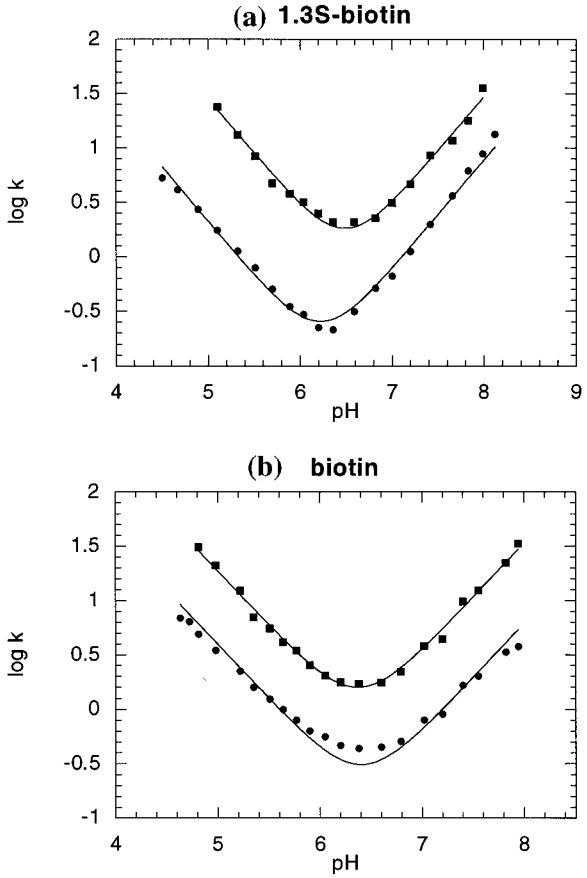

FIGURE 4: log *k* vs pH graphs for (a) holo-1.3S−biotin and (b) free biotin in 90% H_2O/10% D_2O (v/v) at 20 °C. The lines through ■ for NH1′ and through ● for NH3′ are nonlinear least-squares fits of pH dependence of the biotin ureido NH proton exchange data to eq 5. T_1 values and the exchange rates obtained are given in Table 2.

The T_1 relaxation times of NH1′ and NH3′ for the protein-bound biotin are 0.95 and 0.85 s, respectively, compared to the values of 1.90 and 1.80 s for free biotin. The observed relaxation times for biotin on the protein show that as expected its motion is restricted when it is linked to the protein. However, the NH1′ and NH3′ relaxation times are significantly larger than the relaxation time of protein backbone amides (0.4−0.5 s) indicating that the moiety still retains considerable mobility or flexibility.

Variable Temperature Studies. ^{1}H NMR data were obtained in the temperature range from 5 to 50 °C for the holo-1.3S protein and for free biotin. No major changes were observed in the protein chemical shifts, which indicate that significant structural changes in the protein did not occur. The chemical shifts of the two ureido-ring protons of biotin changed linearly over the entire temperature range analyzed. The temperature coefficients of amide proton chemical shifts ($\Delta\delta/\Delta T$) values are −5.8 and −6.7 for NH1′ and NH3′ protons, respectively, for both free and protein-bound biotin (Table 2). For free biotin the $\Delta\delta/\Delta T$ values are similar to those reported by Fry et al. (*14*). Again, this suggests that the environment about the ureido NHs is similar for free and protein-bound biotin and that strong protein−biotin interactions, steric or hydrogen-bonding, are absent. Further, the observed linearity in the $\Delta\delta$ down to 5 °C suggests that the NH protons are not involved in interactions even at low temperatures.

Similarities between the Holo- and Apo-1.3S Proteins

Proton 1D and 2D ^{1}H−^{1}H homonuclear DQF-COSY, TOCSY, and NOESY experiments were performed on the apo-1.3S protein under similar conditions to those used for the holo-1.3S protein. The amide proton regions of the ^{1}H 1D spectra for the apo- and holo-proteins are compared in Figure 2. Expanded fingerprint regions of the 2D TOCSY overlayed spectra of the holo- and apo-proteins are shown in Figure 5. The striking similarities in the 1D and 2D spectra for the holo- and apo-forms strongly suggest that the protein fold is identical for the holo- and apo-1.3S proteins.

Differences in the Biotin Environments in the 1.3S and in the Biotin Carboxyl Carrier Protein

Recently, Athappilly and Hendrickson (*27*) determined the crystal structure of a fragment (corresponding to residues 77−156 in the intact protein) of the biotin carboxyl carrier protein ($BCCP_{sc}$), the biotinyl subunit found in *E. coli* acetyl-CoA carboxylase. The fold of $BCCP_{sc}$ comprises two sets of four antiparallel β-strands, $\beta1-\beta8$. It may be described as a capped β-sandwich, and has a quasi-dyad symmetry. Each symmetry half contains a "hammerhead" motif, which is a characteristic structural motif of the superfamily of enzymes of biotinyl and lipoyl domains (*27*, *28*). In $BCCP_{sc}$,

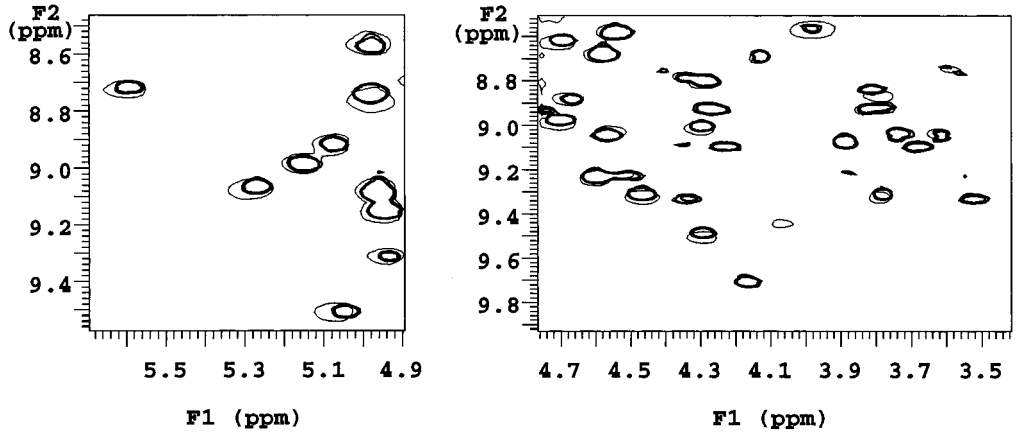

FIGURE 5: Expanded regions of 2D TOCSY overlayed spectra, showing very close structural similarities of holo- and apo-1.3S proteins. The given expanded regions show the through bond correlations in the finger print region of the spectrum. Thick contours for the holo-spectrum and thin contours for the apo-spectrum are used in the display. The spectra were recorded at pH 6.9 for holo- and pH 6.5 for apo-protein in 90% H_2O/10% D_2O (v/v) at 20 °C.

```
                  80        90        100       110       120       130       140       150
                   .         .         .         .         .         .         .         .
Sec.Structure :     BBBBB   BBBB|  thumb |    BBB   BBBBBBBB  BBBBBBBB  BBBBBB     BBB   BBBBBBB
BCCP    (77)  : EISGHIVRSPMVGTFYRTPSPDAKAFIEVGQKVNVGDTLCIVEAMKMMNQIEADKSGTVKAILVESGQPVEFDEPLVVIE      (156)
                  * *|* ||        *| **  |  |* | |* **|||||  *| |   | |  *||     |*  * |* |
TC-1.3S (51)  : KAGEGEIPAPLAGTV       SKILVKEGDTVKAGQTVLVLEAMKMETEINAPTDGKVEKVLVKERDAVQGGQGLIKIG      (123)
Sec.Structure :               BB       BBBBB    BBB   BBBBBBBB   BBBB     BBBBBBB    BBBBBBBBBBB
Prediction                   .                  .         .         .         .         .
                            60                 70        80        90       100       110       120
```

FIGURE 6: Sequence alignment between $BCCP_{sc}$ and 1.3S proteins. The letter "B" indicates the β-strands in $BCCP_{sc}$ and the predicted β-sheet structure in 1.3S by secondary structure predictions. The residue numbering in the respective sequences are given above and below the sequences. The region corresponding to the thumb-like structure in $BCCP_{sc}$ between residues 93 and 102 is labeled as "thumb" above the sequence. In the sequences marked "|" and * indicate identical and similar residues, respectively. The alignment was done using the SEQSEE program (*33*).

the biotinylated lysine 122 is located at a hairpin β-turn between β4 and β5 connecting the N-terminal and the C-terminal halves. The biotin group is partially buried in the surface of $BCCP_{sc}$, with the ureido ring positioned between the protein core and a "thumb-like" protrusion formed by residues 94 and 101. In the present context, the "thumb" and its association with biotin is the most intriguing feature of this structure. It renders the ureido ring protons largely inaccessible from the solvent, with the NH1′ being completely buried. Several protein groups (Tyr 92-Pro 97, Ile 117) are located within 5 Å of the biotin moiety. Further, the structure exhibits very specific interactions between the ureido ring and the protein moiety in this region. Two hydrogen bonds are formed between the side-chain -OH and main-chain oxygen atoms of Thr 94 with the ureido carbonyl (O2′) and N1′-H atoms of biocytin, respectively.

Interestingly, our results provide no evidence for a strong interaction between biotin and the protein in 1.3S−biotin complex. A comparison of the chemical shifts, temperature coefficients $\Delta\delta/\Delta T$ values, and amide proton exchange rates as well as relaxation experiments for free biotin and protein-bound biotin indicates that the biotin on holo-1.3S protein has little interaction with the protein. Furthermore, in the 2D NOESY spectrum of the holo-1.3S protein (Figure 3a,b), no NOE cross peaks were observed between the biotin NHs and the protein and thus there are no indications of hydrogen bonding between the ureido ring and protein backbone and/or side-chain groups. Thus, it appears that the biotin is in different environments in $BCCP_{sc}$ of *E. coli* acetyl-CoA carboxylase and in 1.3S of transcarboxylase. One obvious difference is that the X-ray results on $BCCP_{sc}$ pertain to the solid phase, while the present NMR results address the conformation in solution.

Structure-based sequence alignments (*27, 28*) as well as other multiple sequence alignments (*29, 30*) showed that the overall fold of biotinyl and lipoyl domains is similar. Thus, these proteins seem to form a superfamily of enzymes. Similarly, a direct alignment of $BCCP_{sc}$ and TC 1.3S (Figure 6) and a sequence identity of 30% supports the suggestion that structurally these two domains will have the same overall fold. In particular, the β-strands in the structure of $BCCP_{sc}$ align well with β-sheet structure in 1.3S predicted by secondary structure prediction algorithms (*31, 32*). However, it can be seen that the alignment is good only in the C-terminal part of the two proteins. The N-terminal protein halves, especially between residues 51−72 for 1.3S and 77−105 in $BCCP_{sc}$, exhibit only low similarity (18%) and a 7-residue deletion occurs in 1.3S. In $BCCP_{sc}$ this region includes the "thumb" like structure which is interacting with biotin. The shown alignment (Figure 6) is dependent on the chosen alignment parameters, but multiple sequence alignments of $BCCP_{sc}$, 1.3S, as well as four other biotinylated domains (data not shown) using SEQSEE (*33*), and published sequence comparisons (*27*) also indicate the possibility of deletions occurring in this sequence region in various members of the superfamily. These observations suggest that polar residues such as Thr 94 in $BCCP_{sc}$ might not be suitably positioned to hydrogen bond with biotin in 1.3S. Also, it is possible that the entire "thumb" like protrusion observed in $BCCP_{sc}$ might not exist in other members of the superfamily such as 1.3S, which would explain our experimental observation that the biotin in 1.3S is not interacting with the protein. The relevance of these structural differences between $BCCP_{sc}$ and 1.3S to biotin activation is not clear. The observed intramolecular interactions between protein and biotin moieties in $BCCP_{sc}$ are not necessarily relevant for enzyme catalysis, as the enzyme is also functional (albeit with significantly reduced activity) with biotin as a non-covalent cofactor. Further, one could speculate that the local biotin conformation has to significantly change to allow for carboxylation of the largely buried ureido ring.

Relevance of NH Exchange Rates of 1.3S TC to Mechanism

An important observation concerns the pH profile for the rates of exchange of the NH1′ proton seen in Figure 4. The pH profile for biotin bound to 1.3S shows a strong similarity to that for free biotin. This raises an interesting issue regarding the carboxylation mechanism for biotin in TC in its optimal pH range for activity, which is between pH 5.5−6.5 (*30, 34*). To explain the reactivity of the N1′ ureido atom toward CO_2, Knowles (*13*) postulated that the reactive N^- species is generated by base catalysis at a rate comparable to that seen for the overall turnover rate for TC. This may indeed be true for 1.3S at pHs above 7.5 (Figure 4). However, from the second-order rate constant for base-catalyzed exchange, 4.3×10^7 M^{-1} s^{-1} (Table 2), we can calculate the rate of formation of the $N1'^-$ species to be between 0.14 and 1.4 s^{-1} between pH 5.5 and 6.5, respectively. These rates are considerably less than the turnover rate of ~66 s^{-1} measured for TC (*30, 34*). In the pH range of optimal activity we see that acid-catalyzed exchange predominates, but Perrin and Dwyer (*15*) have eliminated this as a possible mechanism to activate the N1′ atom for attack on a CO_2 group or molecule. Using the second-order rate constant of 5×10^2 M^{-1} s^{-1}, the rate of formation of a protonated reactive isourea form of the ureido ring (*15*) is calculated to be 1.6×10^{-3} s^{-1} at pH 5.5. Thus, neither the base-catalyzed generation of $N1'^-$ nor the acid-catalyzed

formation of an isourea-like species can generate a species fast enough to account for the reactivity of the N1′ nitrogen in intact TC. Therefore, the means by which N1′ is activated for the nucleophilic attack of the carboxyl group of methylmalonyl-CoA remains an open question.

CONCLUSIONS

In this study no evidence was found for significant interactions between biotin and its 1.3S carrier protein. Moreover, contrary to Knowles' proposal (*13*), in 1.3S base-catalyzed generation of a N1′ negative species occurs too slowly to account for the reactivity of biotin toward CO_2 in the holoenzyme at the physiological pH in propionic acid bacteria. Together these two findings lead to the notion that activation of the N1′ atom occurs at the interface between 1.3S and its substrate-bearing 12S partner.

ACKNOWLEDGMENT

The authors like to thank Dr. S. Rothemund for many helpful discussions.

REFERENCES

1. Bonjour, J.-P. (1985) *Ann. N.Y. Acad. Sci. 447*, 97−104.
2. Wood, H. G., and Kumar, G. K. (1985) *Ann. N.Y. Acad. Sci. 447*, 1−22.
3. Shenoy, B. C., and Wood, H. G. (1988) *FASEB J. 2*, 2396−2401.
4. Sauers, C. K., Jencks, W. P., and Groh, S. (1975) *J. Am. Chem. Soc. 97*, 5546−5553.
5. Stallings, W., Monti, C. T., Lane, M. D., and DeTitta, G. T. (1980) *Proc. Natl. Acad. Sci. U.S.A. 77*, 1260−1264.
6. Tipton, P. A., and Cleland, W. W. (1988) *J. Am. Chem. Soc. 110*, 5866−5869.
7. DeTitta, G. T., Edmonds, J., Stallings, W., and Donohue, J. (1976) *J. Am. Chem. Soc. 98*, 1920−1926.
8. DeTitta, G. T., Blessing, R. H., Moss, G. R., King, H. F., Sukumaran, D. K., and Roskiwitalski, R. L. (1994) *J. Am. Chem. Soc. 116*, 6485−6493.
9. Berkessel, A., and Breslow, R. (1986) *Bioorg. Chem. 14*, 249−261.
10. Chen, C., Parthasarathy, R., and DeTitta, G. T. (1976) *J. Am. Chem. Soc. 98*, 4983−4990.
11. Kluger, R., Davis, P. P., and Adwadkar, P. D. (1979) *J. Am. Chem. Soc. 101*.
12. Thatcher, G. R. J., Poirier, R., and Kluger, R. (1986) *J. Am. Chem. Soc. 108*.
13. Knowles, J. R. (1989) *Annu. Rev. Biochem. 58*, 195−221.
14. Fry, D. C., Fox, T. L., Lane, M. D., and Mildvan, A. S. (1985) *J. Am. Chem. Soc. 107*, 7659−7665.
15. Perrin, C. L., and Dwyer, T. J. (1987) *J. Am. Chem. Soc. 109*, 5163−5167.
16. Shenoy, B. C., Magner, W. J., Phillips, N. F. B., Kumar, G. K., Hasse, F. C., and Samols, D (1993) *Protein Expression Purif. 4*, 85−94.
17. Rance, M., Sørensen, O. W., Bodenhausen, G., Wagner, G., Ernst, R. R., and Wüthrich, K. (1983) *Biochem. Biophys. Res. Commun. 117*, 479−485.
18. Piantini, U., Sørensen, O. W., and Ernst, R. R. (1982) *J. Am. Chem. Soc. 104*, 6800−6801.
19. Braunschweiler, L., and Ernst, R. R. (1983) *J. Magn. Reson. 53*, 521−528.
20. Davis, D. G., and Bax, A. (1985) *J. Am. Chem. Soc. 107*, 2820−2821.
21. Jeener, J., Meier, B. H., Bachmann, P., and Ernst, R. R. (1979) *J. Chem. Phys. 71*, 4546−4553.
22. Kumar, A., Ernst, R. R., and Wüthrich, K. (1980) *Biochem. Biophys. Res. Commun. 95*, 1−6.
23. Macura, S., and Ernst, R. R. (1980) *Mol. Phys. 45*, 95−117.
24. O'Neil, J. D. J., and Sykes, B. D. (1989) *Biochemistry 28*, 6736−6745.
25. Smallcombe, S. H. (1993) *J. Am. Chem. Soc. 115*, 4776−4785.
26. Ikura, M., and Hikichi, K. (1982) *Org. Magn. Reson. 20*, 266−273.
27. Athappilly, F. K., and Hendrickson, W. A. (1995) *Structure 3*, 1407−1419.
28. Brocklehurst, S. M., and Perham, R. N. (1993) *Protein Sci. 2*, 626−639.
29. Samols, D., Thornton, C. G., Murtif, V. L., Kumar, G. K., Hasse, F. C., and Wood, H. G. (1988) *J. Biol. Chem. 263*, 6461−6464.
30. Shenoy, B. C., Xie, Y., Park, V. L., Kumar, G. K., Beegen, H., Wood, H. G., and Samols, D (1992) *J. Biol. Chem. 267*, 18407−18412.
31. Rost, B., and Sander, C. (1993) *J. Mol. Biol. 232*, 584−599.
32. Rost, B., and Sander, C. (1994) *Proteins 19*, 55−72.
33. Wishart, D. S., Boyko, R. F., Willard, L., Richards, F. M., and Sykes, B. D. (1994) *Comput. Appl. Biosci. 10*, 121−132.
34. Wood, H. G., Chiao, J. P., and Poto, E. M. (1977) *J. Biol. Chem. 252*, 1496−1499.

BI971674Y